
Article:
Stansfield, Ekaterina, Evteev, Andrej and O'Higgins, Paul orcid.org/0000-0002-9797-0809 (2018) Can diet be inferred from the biomechanical response to simulated biting in modern and pre-historic human mandibles? Journal of Archaeological Science: Reports. ISSN 2352-409X

https://doi.org/10.1016/j.jasrep.2018.07.019

Can diet be inferred from the biomechanical response to simulated biting in modern and pre-historic human mandibles?

Ekaterina Stansfield[1] , Andrej Evteev[2] and Paul O'Higgins[1]

[1]Ekaterina Stansfield (corresponding author)
Hull York Medical School and Department of Archaeology of the University of York
John Hughlings Jackson Building, University of York, Heslington, York YO10 5DD, UK
ekaterina.stansfield@york.ac.uk

[1]Paul O'Higgins
Hull York Medical School and Department of Archaeology of the University of York
PalaeoHub, Wentworth Way, University of York, Heslington, York YO10 5DD, UK
paul.ohiggins@hyms.ac.uk

[2] Andrej Evteev
Research Institute and Museum of Anthropology, Moscow State University,
11 Mokhovaya Street, Moscow, 125009, Russian Federation
evteandr@gmail.com

Key words: Biomechanics, mandible, form and function, Upper Palaeolithic, Mesolithic, FEA, dietary inference.

Abstract

Differences among mandibular remains of past and present populations might be expected to reflect differences in loading history and so, diet. This is because evolutionary and experimental studies and orthodontic observations in modern humans indicate that adult mandibular form is influenced by genetic and loading history. In this study, we apply geometric morphometrics and biomechanical modelling to the mandibles of Upper Palaeolithic, Mesolithic hunter-gatherers and recent and living humans in order to assess if and how differences in adult form reflect subsistence strategies and so, masticatory system loading history. We show, using analyses of size and shape variation, that mandibular form in humans varies in a way that is consistent with the differences among subsistence groups. In particular mandibles from individuals who habitually fed on prepared and softened foods are small and show relative shortening of the mandibular body, among other differences. Using finite element analysis to simulate central incisor and first molar loading, we demonstrate that the performance of the human mandible in terms of resisting deformation covaries with mandibular form (size and shape). However, biomechanical performance in incisor or molar bites reflects only a proportion of the total variance in mandibular morphology; different aspects of morphology contribute to resisting different bites. Nevertheless, differences in biomechanical performance do reflect subsistence mode to some extent, especially for anterior bites. These differences are most strongly associated with mandibular size, the relative length of the body and the form of the gonion; which in turn reflect the degree of mandibular development, and so, loading history. While small, modern mandibles are more efficient at converting muscle to biting forces because of their shortened out lever arm (the body) they are not as capable of withstanding these loads and, for the same input force, deform more relative to upper Palaeolithic and Mesolithic individuals. Thus, we conclude that the differences between modern and prehistoric humans principally arise due to reduced mandibular loading during ontogeny rather than as adaptations to softer diets; they reflect underdevelopment. As such, it is unlikely that morphological and functional comparisons of mandibles across cultural transitions can differentiate anything other than broad aspects of loading history at a population level.

1. Introduction

Differences in craniofacial morphology between pre-historic hunter-gatherers and agricultural populations have led to the view that diet has a significant impact on aspects of craniofacial form. In particular, shifts in cranial morphology have been shown to be associated with cultural change in populations worldwide, e.g. in South America, the Ohio Valley, Nubia and Southern Levant (Carlson and Van Gerven, 1977; González-José et al., 2005; Pinhasi et al., 2008; Paschetta et al., 2010). In modern humans, malocclusion and a higher prevalence of dental crowding have been recorded in post-industrial urban populations and linked to the reduced duration and intensity of mastication (Corruccini, 1984) due to processing, preparing and cooking foods. Rando et al. (2014) reported differences in mandibular morphology between mediaeval and post-mediaeval periods in London when food items became softer. Statistically significant reductions were observed in nearly all measurements of post-mediaeval mandibles, including the gonial angle, ramus height and width, bi-gonial breadth and bi-condylar breadth. Differences were noted to be greatest in regions of attachment of masticatory muscles. A study by Mays (2015) of two populations from the north-west of Europe, one from Zwolle (The Netherlands, 19th century CE) and the other from Wharram Percy (England, 10th–19th century) reported a similar pattern. These authors used the rate of tooth wear as a proxy for the toughness of the diet and shown that the population from Wharram Percy, whose rate of tooth wear was higher, also possessed more robust mandibles.

Several experimental studies in animals show that the degree of masticatory loading during ontogeny influences the development of mandibular form. Thus, Kono et al. (2017) fed mice on a powdered soft-diet (SD) or hard-diet (HD) of regular rodent pellets from the 3rd to 9th weeks of life and then Micro-CT scanned them. They found pronounced under-development of the proximal body of the mandible, the angular process and the condyles in the soft-diet mice. An equivalent study with similar findings was earlier reported by Hichijo et al. (2014) in mole rats and Bozzini et al. (2015) in common rats. Other animals, such as the rock hyrax (Lieberman et al. 2004), minipigs (Ciochon et al. 1997) and rabbits (Menegaz et al. 2010; Ravosa et al. 2010) brought up on softer, more processed food experienced less growth in the mandible, lower face and zygomatic region than those that were given fresh, unprocessed food items. Additionally, Spassov et al. (2017) have noted that cranial skeletal form is altered in mice with congenital muscle dystrophy and by diet consistency. It can therefore be expected that humans also display plasticity of the masticatory apparatus such that it adapts ontogenetically to the loads placed upon it. As such mandibular form can be expected to reflect loading history.

Differences in mandibular morphology among human populations can also be attributed to different histories and genetic drift. For example, Nicholson and Harvati (2006) found that modern human mandibular shape exhibits considerable geographic patterning, with some aspects of mandibular morphology reflecting a climatic gradient, and others, functional specialization. Nevertheless, Smith (2009) demonstrated that genetic distances between populations provide a poor explanation of observed variations in the shape of the mandible. In a later study, von Cramon-Taubadell (2011) found that habitually agricultural/pastoralist populations, irrespective of their geographical location, and therefore genetic proximity, tend to have 'relatively shorter and broader mandibles with (relatively) taller and more angled rami and coronoid processes. At the same time, foraging populations have (relatively) longer and narrower mandibles with short and upright rami and coronoid processes' (Cramon-Taubadel, 2011 p. 19547).

From an archaeological point of view, one needs to ask whether the morphology of the human masticatory apparatus is indicative of its loading from birth to adulthood (loading history) and so, diet since an association between morphology and diet does not necessarily imply causation. For example, Menendez et al. (2014) found that, although southern South American human cranial variation in size and shape was significantly correlated with diet composition, the bite forces, estimated from the attachment surface areas and lever mechanics of masseter and temporalis muscles , did not explain the pattern of morphological variation among the analysed samples, when assessed with regression analysis. In their study, Menendez et al. (2014) assumed that muscle attachment surface area is indicative of the bite forces, following some earlier methodological developments in animals by Kiltie (1984) and Thomason (1991). However, Toro-Ibacache et al. (2016a) found only a weak association between the cross-sectional area of the temporalis muscle and cranial form, even though Weijis and Hillen (1986) determined it that the cross-sectional areas of temporalis and masseter muscles correlate positively with facial width and areas of masseter and pterygoid muscles correlate significantly with mandibular length.

When the evidence is taken as whole, it is still not clear to what extent and in what ways diet, and so the mechanical loading history of the masticatory system, underlies the differences in morphology among human subsistence groups. One potential test is to assess the extent to which mandibles associated with more processed diets are more or less effective at processing food items. The expectation is that when diets are less processed/softened, as was the case for Upper Palaeolithic and Mesolithic populations, the resulting mandibles are better able to generate and resist high bite forces than modern mandibles that have experienced softer diets during their development. Wroe

et al. (2010) tested the hypothesis that the modern human bite is weak and the skull is unable to sustain bite forces of the same magnitudes as can be achieved by other hominoids. They applied three-dimensional finite element analysis to the cranium and mandible of a modern human, several extant hominoids and two early representatives of the hominin radiation: *Australlopithecus africanus* and *Paranthropus boisei*. They, observed that humans produce higher bite forces in comparison with other hominoids when all specimens are scaled to the same size. This suggested that the human skull was optimized to produce relatively larger magnitudes of bite force when applying smaller muscle forces than our ancestors and relatives. This is the opposite of what might be expected from a consideration of diet and points to dissociation between the demands of food processing and the ability to generate and resist bite forces.

In the present study, we assess the extent to which mandibular morphological variation among Upper Palaeolithic, Mesolithic, recent and living humans, i. reflects loading history and so diet and ii. reflects adaptation to softer diets in more modern populations rather than failure to fully achieve their growth potential because of reduced loading. . We approach these questions by testing the following null hypotheses.

$H1_0$: Mandibular form does not vary in a way that is consistent with the differences described among modern subsistence groups.

If this is falsified we then investigate the extent to which differences in mandibular form translate into differences in performance (bite forces and skeletal deformations in simulated bites)

$H2_0$: Performance does not covary with mandibular form.

If this hypothesis is falsified we consider the extent to which differences in mandibular functional performance reflect differences in food processing. The expectation is that mandibles from populations with less processed diets should be more efficient at converting muscle into biting forces and in resisting biting and muscle forces.

$H3_0$: If $H2_0$ is falsified, differences in form and performance are consistent with differences in diet.

If this is falsified we will have shown that the morphology of modern mandibles from individuals raised on more processed diets is not a consequence of adaptation but more likely reflects other factors, including failure to fully develop (achieve their growth potential).

2. Material and Methods

2.1. Raw data

The raw data comprise CT scans of mandibles of two Upper Palaeolithic modern humans, 6 Mesolithic individuals from the Ukraine ('Ukr Meso'), 6 Mesolithic individuals from Schela Cladovei ('Schela'), Romania, six mandibles from Kozino, Russia that date from the XVIII century ('Modern small') and a large (relative to the material from Kozino) contemporary modern Russian male from Moscow (clinical CT) ('Modern large') , all males with the full dentition present (Table 1). All CT scans were re-sampled with voxel size of 0.5, 0.5, 0.5 (mm) to ensure models are comparable.

Table 1. Mandible CT scans.

Tag	Name	Time and culture group	Number	Provenance	Resolution (mm)
Oase	Oase 1	Upper Palaeolithic (12% Neanderthal hybrid), Romania	1	Romania, courtesy Prof E. Trinkaus	0.40, 0.40, 0.40
Sungir	Sungir 1	Upper Palaeolithic, Russia	1	Russia, courtesy of Dr S. Vasiliev	0.43, 0.43, 0.25
Schela	Schela Cladovei	Mesolithic, Romania	6	Romania, courtesy of Dr A. Soficaru	0.48, 0.48, 0.60
Ukr Meso	Vasilievka 1, Voloshskoe	Mesolithic, Ukraine	6	Courtesy Prof A Buzhilova	0.43, 0.43, 0.25
Modern small	Kozino	XVIII century, Russia	6	Courtesy Prof A Buzhilova	0.43, 0.43, 0.25
Modern large	n/a	living, Russia	1	Courtesy Prof A Buzhilova	0.47, 0.47, 0.30

Representatives of archaeological groups in this study are derived from pre-pottery periods in the region. Thus, the Oase humans (Pescera cu Oase, Romania) individuals have been dated to 37,000-42,000 years BP (Fu et al., 2015) and Sungir 1 (Vladimir Oblast, Russai) is dated to 30,000 years BP (Nalawade-Chawan et al., 2014). These individuals are believed to have derived a large proportion of their nutrition from hunting ruminants in peri-glacial steppe or forested environments (Hoffecker, 2002).

The Mesolithic groups from Schela Cladovei (Danube region, Romania) and Vasilievka/Voloshkoe (Dnieper region, Ukraine) are attributed to Mesolithic (or Epipalaeolithic) groups because of their dating to the end of the last glaciation about 10,000 years BP. It is likely that these people differed in subsistence from the Upper Palaeolithic groups, with high reliance on fresh water resources. Thus, Lille et al. (2011) have shown the importance of freshwater fish in the diet of the Ukranian Mesolithic and Neolithic populations from the Dnieper basin. Similar reports that confirm the fisher-hunter-gathering mode of subsistence for Mesolithic populations of this region relate to material from Lake Onega, north of European Russia (Jacobs, 1995) and the Djerdap Iron Gates region (Lower Danube) (Bonsall et al. 1997, 2000, 2002, 2004, Cook et al., 2001, 2002) where δ 15N and δ 13C ratios were shown to indicate a diet in which almost all protein was derived from river fish. There is no evidence of pottery or usage of domesticated plants in the Danube and Dniester regions at the time of the groups sampled here.

The modern individuals used here are derived from recent urban populations in Russia who relied on a highly processed and soft diet. The chosen individuals span the size range of modern males in the sample, with the large modern mandible matching the size of the Upper Palaeolithic males represented here. The rationale for comparing the large and the small modern individuals with the archaeological sample is in the need to account for differences in size as well as size related shape allometry in the modern individuals.

It is assumed that that the diet of the modern humans required considerably less chewing than those of the pre-pottery Upper Palaeolithic and Mesolithic groups because of food preparation. It is possible that the diet of the fish-reliant Mesolithic people was less mechanically demanding than that the Upper Palaeolithic because cooked fish is a significantly softer than cooked meat. However, this assumes cooking and ignores other aspects/components of diet. However, we do not have sufficient data to say with certainty that the toughness of food in the Upper Palaeolithic and in Mesolithic differed, and if so how. Nevertheless, we choose to divide Upper Palaeolithic and

Mesolithic hunter-gatherers due to the clear difference in the subsistence strategy and it very likely that both of these groups regularly used their jaws to break down tougher foods than those eaten by the modern humans in this study.

2.2. Segmentation, force vectors and spatial constraints of mandibles

All mandibles were segmented as one solid material and then were homogenously and isotropically allocated the material properties of cortical bone in order to control for differences in internal structure and for the influence of segmentation errors. This is based on an extensive sensitivity study carried out as a preliminary to the present work. In this, segmentation was varied by permuting the presence of cancellous bone (as a bulk material), periodontal ligaments and tooth enamel in a series of biting simulations using modern mandibles. These are reported in detail in Stansfield et al. (this issue) and summarised here. Mandibular models were segmented in various ways, by including none, one or two of each of the above structures as separate materials with properties distinct from cortical bone. The muscle vectors were varied through one standard deviation of estimated in a human sample, while spatial constraints varied in the number of voxel nodes that were fixed in space, thus restricting movement of the mandibular condyles and the loaded tooth to greater or lesser degree. The results indicate that potential errors in segmentation and application of muscle force vectors, and constraints can have an appreciable effect on predictions of performance from FEA. However the errors are not large compared to the differences we expect to encounter among specimens in a sample of modern humans.

Thus, in the sensitivity study, all variant models of a single mandible were loaded to simulate incisor or second molar biting. Deformations were compared to those of a sample of 10 mandibles segmented as if all structures have the same material properties as cancellous bone ('solid models') and whose muscle vectors and spatial constraints were kept the same. It was found that the variance among these 10 different individuals was considerably larger than the variance in one individual resulting from different muscle vectors, spatial constraints and segmentations. Thus, the average variance in von Mises strains due to differences in individual morphology (across 10 individuals) amounts to 6.6×10^{-8} for I_1 and 3.28×10^{-8} for M_2. The average variance in von Mises strains due to segmentation in one individual comprises only 1.9% of the variance among individuals for I_1 and 7.5% of the variance among individuals for M_2 bites. The variance within one individual subject to varying constraints is 3.6% of the inter-individual variance for I_1 and 18% for M_2 bites. At the same time, muscle vector variations in one individual account for 6.2% of the variance among individuals for I_1 bites and 8.3% of the variance among individuals for M_2 bites.

As a result of these studies and for similar reasons to those discussed at length in Fitton et al. (2015), Toro-Ibacache et al. (2016b), and Godinho et al. (2017) we limit the present study to finite element analyses of mandibular models in which the external form of the mandible is accurately represented but the cortical bone, teeth, periodontal ligaments, and cancellous bone as a bulk material are all allocated the same material properties. We keep the applied muscle vectors and spatial constraints the same for all individuals to ensure a fair test of how the shape and size of the mandible alone affect its biomechanical performance in simulated biting. Thus, while it is very likely that different muscle forces were applied to the mandibles in this study in life, we apply the same force to all mandibles in the simulations. This focuses the analysis on the effects of differences in external mandibular form and ignores confounding factors such as differences in applied muscle forces. From the sensitivity study (Stansfield et al, this issue) we know that differences in applied force magnitudes will mainly impact the degree of deformation and differences in relative activation, the mode. The impact of these is additional to the impact of differences in form and is substantially smaller. Thus the likely impacts of differences in muscle forces and relative activation are considered in the discussion rather than experimentally. It is not possible to apply accurate forces because we cannot estimate them with any reliability (Toro-Ibacache et al, 2015) from cranial skeletal morphology; nor is it desirable from the point of view of the experimental design. Thus, this approach greatly simplifies reality and allows the analyses to focus on differences in biomechanical response due to a single variable, the form of the mandible while holding all other variables constant. In consequence, our FEAs do not aim to estimate actual performance in mandibles but rather to assess the impact of size and shape differences on performance, while holding all other potential sources of variation constant.

2.3. Models for the finite element analyses

The number of voxel elements in each mandibular FE model varied because of the differences in the size and shape of the models ranging from 461,250 to 682,127. As noted above, the segmentation was carried out to produce solid models of mandibles and teeth with homogenous and isotropic material properties of cortical bone (Young's modulus of 17 GPa and Poisson's ratio of 0.3; Gröning et al, 2011a).

To ensure comparability of loading, all models were translated and rotated such that their occlusal plane (defined here, because teeth are variably present, by the triangle of landmarks, infradentale, alveolar process posterior buccal right and alveolar process posterior buccal left) coincided with the

x>0, y>0, z=100 plane. The positions of the right and left condyles were fixed by constraining 60 nodes on their antero-central portions in x, y, and z directions. The loaded tooth, i.e. the first right incisor or the second right molar, was constrained only in the vertical (z) direction. Identical muscle forces and muscle activation patterns based on those used by Gröning et al. (2011b), Table 2, were applied to each mandible to simulate unilateral bites on the right central incisor or the right second molar. The muscle force vector directions were identical for each model. These were obtained in advance as average directions of vectors from the centroid of the muscle insertion on the mandible to the centroid of the muscle origin on the skull for nine modern individuals. These vectors were then translated to the centroids of the muscle insertions to fit each of the models (Table 2 and Fig. 1). The analysis was carried out using the FEA software tool VoxFe (the latest version of which is available at https://sourceforge.net/projects/vox-fe/).

Table 2. Maximum muscle forces and scaling factors for different bites**

	Maximum	**Incision**		**Molar**	
	force	left	right	left	right
Superficial masseter	218	0.4	0.4	0.6	0.72
Deep Masseter	112	0.26	0.26	0.6	0.72
Anterior temporalis	168	0.08	0.08	0.58	0.73
Middle temporalis	137	0.06	0.06	0.67	0.66
Posterior temporalis	119	0.04	0.04	0.39	0.59
Medial pterygoid	192	0.78	0.78	0.6	0.84
Inferior lateral pterygoid	90	0.71	0.71	0.65	0.3

**Groening et al (2013).

Figure 1. Finite element model of a mandible showing muscle attachment areas (masseter, dark blue = deep, light blue =superficial; temporalis, anterior = pink, middle = red, posterior = brown; medial pterygoid = violet; lateral pterygoid = rose). Lines of action are drawn between origin and insertion, condylar and incisor constraints shown in black (see text for details).

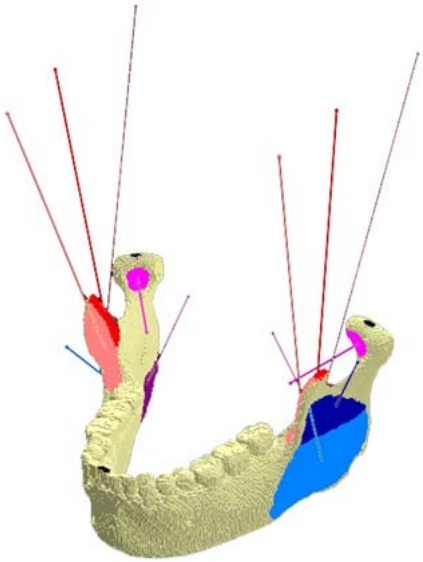

2.4. Geometric morphometric analysis

The shapes and sizes of the mandibles were quantified using 33 fixed landmarks and 215 semilandmarks on curves and surfaces (Table 3) using the EVAN Toolbox software (http://www.evan-society.org). The landmark and semilandmark data of the Mesolithic individuals from Schela and Ukr Meso were also used to calculate group average forms for each site to be employed in some of the subsequent analyses. These were converted to FE models by warping the surface of one individual to fit the mean landmark coordinates in each group. The choice of the surface was made on the basis of typicality, state of preservation and the presence of all three molars on both sides in occlusion. The warped surfaces were then converted to voxel stacks using Avizo (Thermo Scientific™) for subsequent analyses.

Table 3. Landmarks and semilandmarks

Fixed landmarks	**Semilandmarks**	
01_Gnathion	Name	Number
02_Infradentale	Curve01_LowerBorderLeft	10

03_Linguale	Curve02_LowerBorderRight	10
04_Orale mandibular	Curve03_MandibularNotchLeft	10
05_Pogonion	Curve04_MandibularNotchRight	10
06_C-P_3 left	Curve05_RamusAnteriorLeftCurve	10
07_C-P_3 right	Curve06_RamusAnteriorRightCurve	10
08_P_4-M_1 left	Curve07_RamusPosteriorLeftCurve	8
09_P_4-M_1 right	Curve08_RamusPosteriorRightCurve	8
10_M_1-M_2 left	Curve09_SaggMentAnterior	4
11_M_1-M_2 right	Curve10_SaggMentPosterior	5
12_mental foramen anterior left	Patch01_AlveolarProcessPosteriorLeft	5
13_mental foramen anterior right	Patch02_AlveolarProcessPosteriorRight	5
14_alveol proc bucc posterior left	Patch03_BodyPosteroMedialSurfaceLeft	5
15_alveol proc bucc poster right	Patch04_BodyPosteroMedialSurfaceRight	5
16_ramus root left	Patch05_bodyAnteriorSurfaceLeft	13
17_ramus root right	Patch06_bodyAnteriorSurfaceRight	13
18_gonion left	Patch07_bodyPosteriorSurfaceLeft	10
19_gonion right	Patch08_bodytPosteriorSurfaceRigh	10
20_Lateral condyle left	Patch09_ramusLeft	10
21_Lateral condyle right	Patch10_ramusRight	10
22_Central condyle left	Patch11_ramusPosteriorLeft	22
23_Central condyle right	Patch12_ramusPosteriorRigh	22
24_Medial condyle left		
25_Medial condyle right		
26_Sigmoid notch left		
27_Sigmoid notch right		
28_Coronion left		
29_Coronion right		
30_mandibular foramen inferior left		
31_mandibular foramen inferior right		
32_alveol proc. lingual poster right		
33_alveol proc. lingual posterior left		

Patterns of morphological variation among all individuals and among six mandibular models (Oase, Sungir, Modern large, the smallest of the mandibles from XVIII century Kozino ('Modern small') and

the averages of the two Mesolithic samples, i.e. Schela and Ukr Meso) were assessed by principal component analyses ('PCA') of size and shape variables (shape variables rescaled to the correct centroid sizes for each specimen). We focus on size and shape rather than shape alone because we are concerned to relate patterns of variation to mechanical performance and the latter depends on both size and shape. Size and shape variables were obtained by first carrying out a generalised Procrustes analysis ('GPA') of the six sets of 33 fixed landmarks for Oase, Sungir, Schela, Meso, Modern small and Modern large models (Milne and O'Higgins, 2012; O'Higgins and Milne 2013; O'Higgins et al. 2017) and then multiplying each landmark set by its original centroid size. This is not the quite same approach as that used by Dryden and Mardia (Dryden and Mardia, 1998) to obtain size and shape variables in which unscaled landmarks are translated and rotated. It differs slightly in the eventual rotation among specimens but has the advantage that one can easily move between a size and shape analysis and shape analysis in Kendall's shape space by simply scaling to centroid size 1. The underlying variance structure in shape is preserved in our approach, whereas it is not in the approach of Dryden and Mardia (1998). In any case. differences are slight, a statistical nicety rather than important in terms of these analyses. Note that variances in size and shape scale with size, However, in FEA differences in size and shape due to loading are very small and so this issue is unlikely to impact greatly. However, in general, statistical testing is best carried out after partitioning shape from size, as is conventional in GM studies. Such analyses might examine shape or size differences or shape and size in combination (e.g. the size -shape or 'form space' comprising shape plus natural logarithm of the centroid size; Mitteroecker et al, 2013).

2.5. Analysis of the FEA results

Results of the FEA comprised displacements at each node, von Mises strains throughout the model and the resulting force vectors on each of the constraints. Those on the biting tooth are of interest because they allow us to calculate biting force as the sum of the vertical components of force at the constrained elements. Von Mises strain maps were generated for each model with the same display range to facilitate comparison. Values of displacements and von Mises strains at 248 landmarks and semilandmarks (Table 3) were exported to compare modes and magnitudes of global deformation (see Supplementary materials).

In order to visualise and compare global deformations, the landmark coordinates of unloaded mandibular models and the coordinates of the same landmarks from the loaded models were exported from Vox-Fe. We then followed the protocol developed in previous papers (O'Higgins et

al., 2011, 2012; Milne and O'Higgins, 2012; O'Higgins and Milne, 2013). The coordinates of all unloaded and loaded mandibles were first subjected to GPA and then rescaled to their original centroid sizes to obtain size and shape variables. Next, the differences in landmark coordinates between the loaded and unloaded models were calculated by subtraction. To facilitate the visualisation of results, these were then added to the average unloaded form obtained by averaging the shape variables and multiplying these by the average centroid size. The choice of unloaded model for visualisation does not impact the distances computed among models (or the scatter in a principal component analysis). Finally, to visualise the modes and magnitudes of deformation, a principal component analysis ('PCA') was carried out of the mean unloaded mandibular size and shape together with the new representations of the loaded mandibles referred to this mean.

Partial least squares ('PLS') analyses were performed to assess the degree and nature of any associations between mandibular size and shape and modes and magnitudes of deformation under simulated biting. In these PLS analyses, one block comprises mandibular size and shape variables and the other comprises the sizes and shapes of loaded mandibles

3. Results

3.1. PCA of size and shape, all data.

The first two components in the principal components analysis of the whole dataset account for about 59% of the variance in the sample (Fig. 2a). The first principal component mostly represents variation in mandibular size. It is the second (and higher order components, Figure 2b) that differentiates groups. Here, the two Mesolithic groups and the modern Russian group from Kozino form distinctive clouds, while individual Upper Palaeolithic fossils Sungir and Oase are located at the fringes of the distribution. The large modern Russian sits with the mandibles from Kozino. The tight groupings within the Mesolithic and modern groups justify the use of average models as being typical representatives of distinct groups.

Figure 2. Principal component analysis of the whole dataset. Given that PC1 reflects the dispersion of the sample by size, PC2 v. PC3 are presented to show separation of the groups by the shape of the mandible.

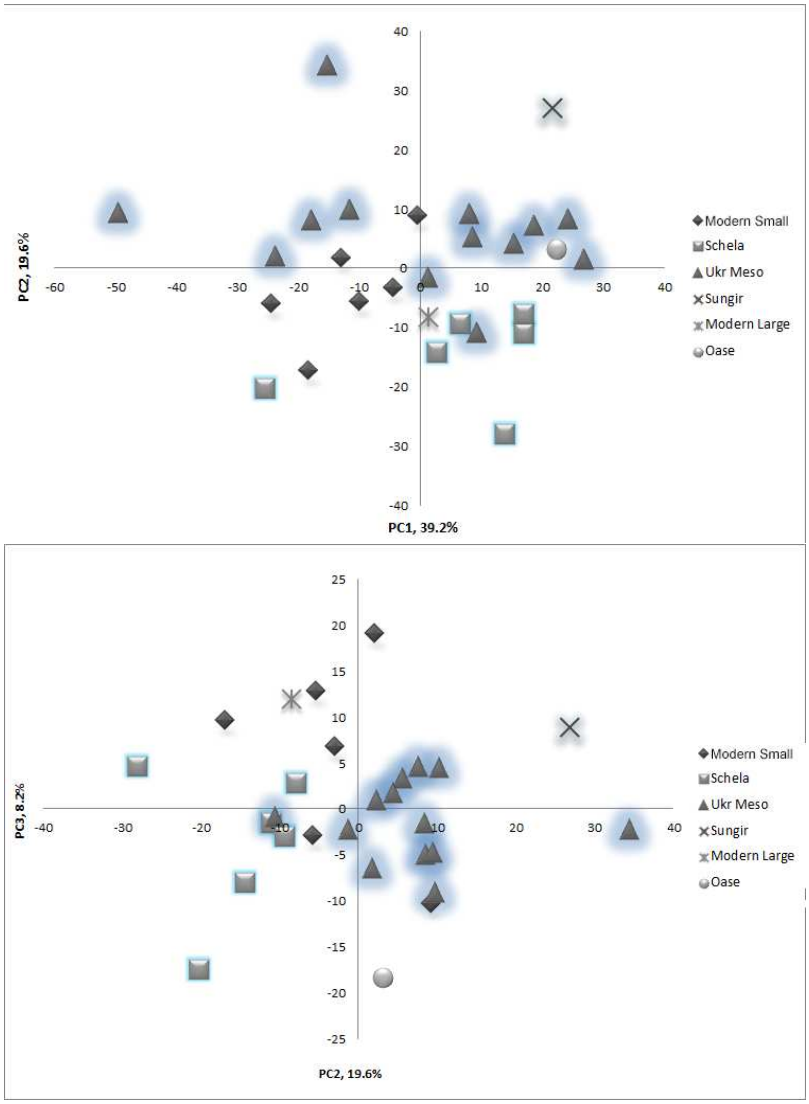

Subsequent analyses reduced the sample size to six models because of the time and effort involved in carrying out FEA. The sample comprised Oase, Sungir, the average mandibles of the two Mesolithic groups, the smallest mandible from the modern Russian group from Kozino and the large mandible of the contemporary Russian man.

3.2. Superimposition of mandibles in the occlusal plane

Figure 3. Mandibles as per key, superimposed (translated and rotated) to best fit the anterior dentition.

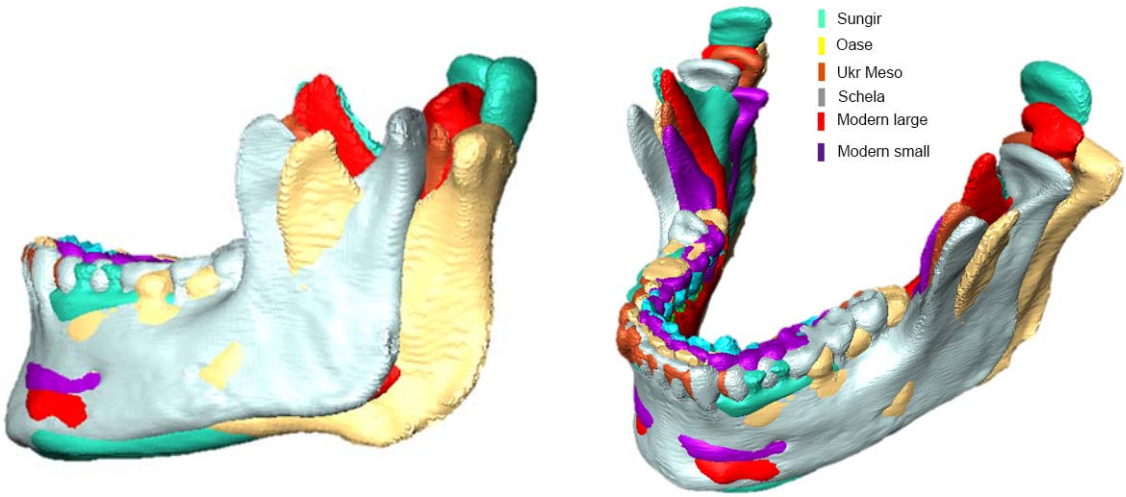

When these 6 models are superimposed in the occlusal plane (Figure 3), registered at the first incisor tips, it is evident that the anterior alveolar process is roughly the same size and shape in all of them regardless of their overall size. The main differences are in (i) the absence of the third molar in the large modern human and (ii) the presence of a small retromolar space in Oase. Form variation is evident as differences in the antero-posterior length of the ramus, the height of the body and ramus and the shape of the gonial angle.

3.3. PCA of size and shape, reduced set of data

The PCA of size and shape of the four individual mandibles and two averages is presented in Fig. 4. The first principal component orders specimens by culture and size. The larger Upper Palaeolithic mandibles are at the positive and the smaller modern mandibles are at the negative extremes of PC1. The inset warpings in Fig. 4 show that PC1, which accounts for 54% of the total variance in size and shape, represents changes in size and in the relationship between the distal dental row and the ascending ramus. Warping the mean to the positive extreme of PC1 (large Upper Palaeolithic mandibles) results in a small retromolar space becoming evident, while at the other extreme of this PC the third molar is tucked behind the ascending ramus. On PC2, which represents 23% of total variance in size and shape, the mandibular ramus varies in (antero-posterior) width and the gonial

angle also varies but the distribution of mandibles on this PC shows no relationship to cultural group or size.

Figure 4. PCA of size and shape of the mandibular sample. PC1 vs PC2, 77.4% of the total variance is displayed in this plot.

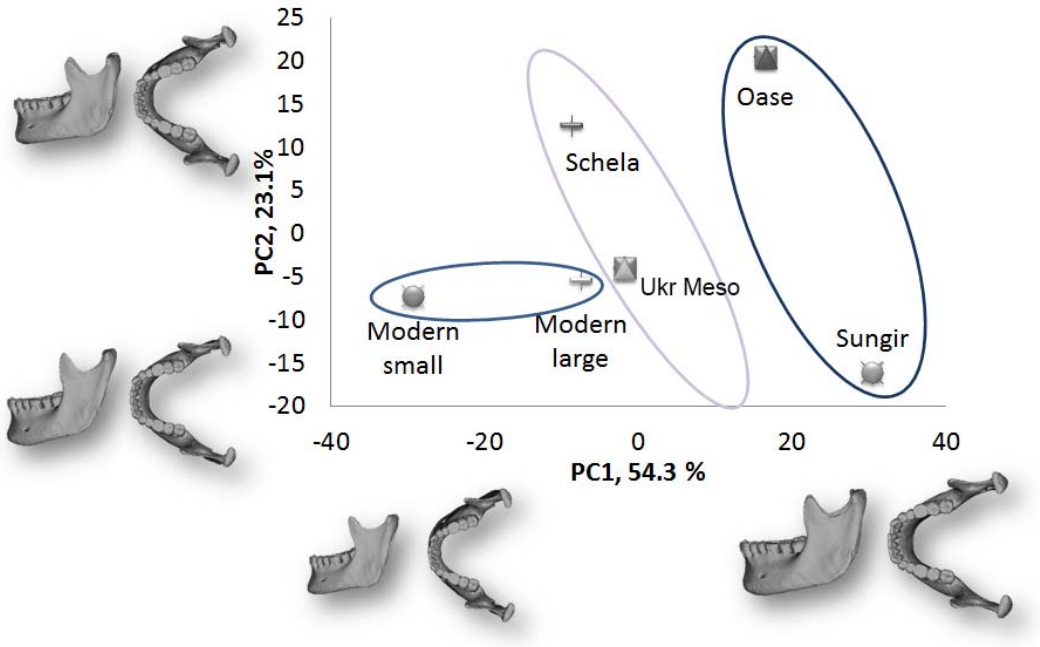

3.4. *Finite element analysis*

3.4.1.Strain maps

All mandibles show similar distributions of regions of high and low von Mises strain during biting simulations (Fig. 5) and this differs between incisor and molar biting. For the incisor bite, the most strained areas are over the alveolus around the loaded tooth, at the condylar neck, at the anterior angle between the ramus and the alveolar process and at the posterior aspect of the mandibular ramus. For the molar bite, the most strained areas are located in the alveolus around the loaded tooth, along the anterior border of the mandibular ramus and in the mandibular notch. Additionally in the molar biting simulations, the small modern human and the Upper Palaeolithic mandibles develop regions of high strain just above the chin.

Figure 5. Von Mises strains developed in each model under simulated incisor and molar biting. See text for details.

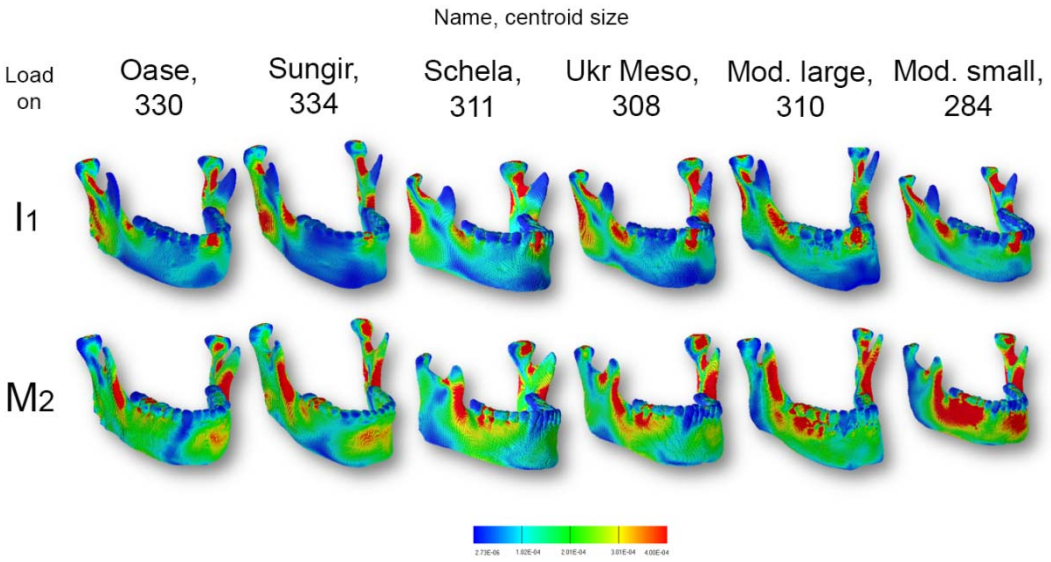

Although the small modern human mandible develops patterns of strain that are similar to those found in the larger mandibles, it clearly experiences considerably larger magnitudes of strain throughout a larger proportion of its body.

3.4.2.Bite force efficiency

The total input muscle force in each bite was the same for all mandibles with the vertical component during the incisor bite equal to 453N and the vertical component during the molar bite equal to 1029N. However, the output (biting) forces are different with the two modern mandibles clearly producing larger bite forces, thus showing greater efficiency (Table 4).

Table 4. Bite efficiency.

	Force on I_1 (N)	**Efficiency in I_1 bite (%)**	**Force on M_2 (N)**	**Efficiency in M_2 bite (%)**
Oase	163.3	36.07	588.9	57.22
Sungir	171.5	37.88	562.8	54.68
Schela	187.0	41.30	674.2	65.50
Ukr Meso	181.6	40.10	619.2	60.16
Russian Large	200.7	44.31	691.3	67.16
Russian Small	227.6	50.27	722.1	70.16

3.4.3.PCA of deformation

A plot of PC1 vs PC2 from the PCA of size and shape variables among the unloaded mean and loaded models is presented in Fig. 6. The inset mandibular surfaces represent the average surface warped to the mean unloaded mandible and to the three most deformed models.

Biting on the incisor results in inward wishboning of the mandibular body, driven by the action of the medial pterygoid muscles. The working side (right), compared to the balancing (left) side experiences greater lateral deflection of the condyle. Mandibles with a longer body, such as the Upper Palaeolithic mandibles of Oase and Sungir, deform (displacement of landmarks) the most (largest size and shape distances from the unloaded model). The smallest overall deformation occurs in the small modern mandible (Fig. 6a).

Figure 6. a) Size and shape analysis of deformations arising from simulated biting on (a) the first right incisor: deformations are visualised as warpings of the mean unloaded model and exaggerated by a factor of 400 to aid visualisation; top left is the unloaded mean mandible, bottom left is deformation in the modern small model, bottom right is the deformation of the Sungir model, and top right is the deformation of the Oase model. b) the second right molar: deformations are visualised as warpings of the mean unloaded model and exaggerated by a factor of 400 to aid visualisation; right inset is the unloaded mean mandible, left top is the deformation in the Sungir model, left middle is the deformation in the Modern small, and left bottom is the deformation in the Modern large models. See text for details.

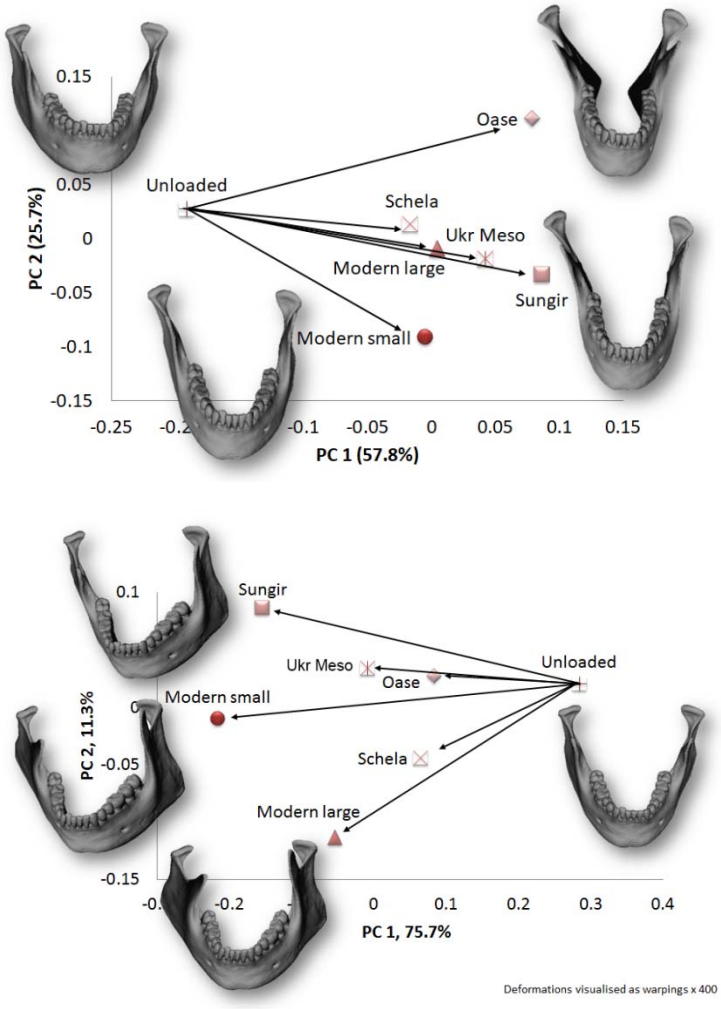

Biting on the second molar results in outward wishboning of the mandibular body coupled with a significant amount of twisting of the working side of the mandible (PC1). This is most pronounced in the modern small mandible from Kozino. In the Sungir mandible at the positive extreme of PC2, the ramus of the working side (right) swings medially relative to the neck and condyle, while the lower border and the gonial angle of the balancing side swings laterally. In the large modern mandible, at the negative extreme of PC2, the gonial angles and body on both sides show pronounced outward wishboning. On the whole, the degree of deformation does not depend on the size of the mandible: the large Oase mandible deforms considerably less than the large Sungir mandible (Fig. 6b).

3.4.4. PLS of deformation and form

Associations between mandibular form and deformation were explored through 2-block partial least squares analyses, PLS for I_1 bites (Fig. 7). The scores of individuals on the resulting first axes (singular

warps) of deformation and size and shape which explain 76% of the total covariance among blocks show a correlation of 0.94 (p= 0.0051). The distribution of models along these axes reflects subsistence group (Fig. 7). These axes explain 49.6% of the total variance in form and 44.4% of the total variance in deformation. The modern mandible that is smaller and has a shorter body undergoes less internal wishboning than larger mandibles with longer bodies and hence longer force lever arms.

Figure 7. PLS of mandibular deformation arising from simulated biting on I_1 (vertical axis) vs. Mandibular size and shape (horizontal axis). The % of the total variance in deformation or form is shown on each axis The correlation between scores on these axes is r= 0.94, P= *0.0051.* Deformations are visualised as warpings of the mean unloaded model to the extremes of each PLS axis and exaggerated by a factor of 400 to aid visualisation.

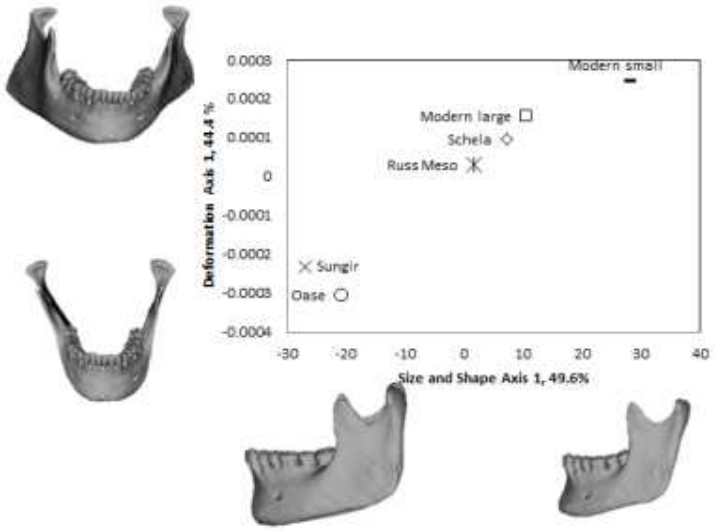

For M_2 bites, the second singular warps (Fig. 8a; axis 2) which explain 13% of the total covariance among blocks are best associated with subsistence group. Scores of individuals on these second axes are strongly correlated r= 0.94 (p= 0.004). Here, 48.1% of the total variance in size and shape, which reflects (inset warpings, bottom of Fig. 8a) size differences and 'squaring' of the angle of the mandible, is associated with variations in the degree of wishboning of the mandibular body (18% of the total variance in deformation; rightmost inset warpings, Fig. 8a). With increasing modernity more obtuse gonial angles and decreasing size, more wishboning occurs.

The first singular warps (axis 1) which explain 75% of the total covariance among blocks from this analysis account for 22% of the variance in size and shape and 49.5% of the variance in deformation.

The correlation between scores on these axes is 0.89 (p= 0.017). Axis 1 the first singular warp of form, distinguishes between narrow mandibles with obtuse gonial angles and open mandibles with square gonial angles, and that of deformation, indicates that narrower mandibles undergo more outward wishboning with a significant lateral twisting of the balancing side (Fig. 8b).

Figure 8. (a) PLS axes 2 of mandibular deformation from simulated biting on M_2 (vertical axis) vs. Mandibular size and shape (horizontal axis). The % of the total variance in deformation or form is shown on each axis. The correlation between scores on these axes is r= 0.94, p=0.004; (b) PLS axes 1 of mandibular deformation (vertical axis) vs. Mandibular size and shape (horizontal axis). The % of the total variance in deformation or form is shown on each axis. The correlation between scores on these axes is r= 0.89, p=0.017. Deformations are visualised as warpings of the mean unloaded model to the extremes of each PLS axis and exaggerated by a factor of 400 to aid visualisation.

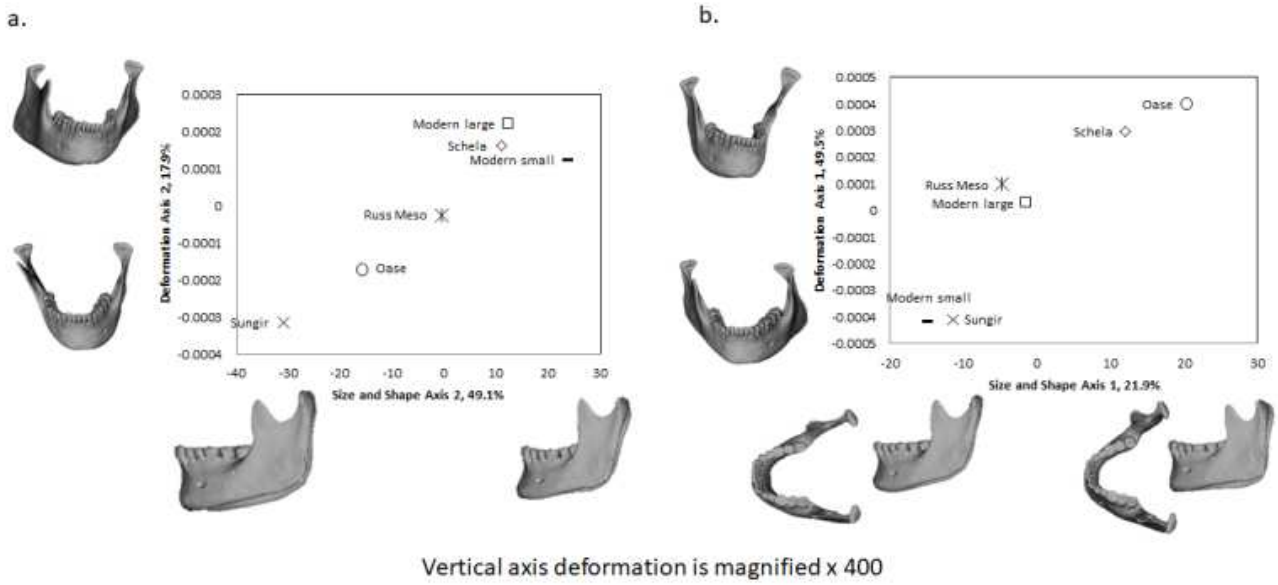

4. Discussion

In this study we examined differences in mandibular morphology and biting performance among pre-historic hunter-gatherers, agricultural populations and recent individuals. In particular, we are interested to study the nature of mandibular variation in size and shape among these groups and to assess the extent to which these differences are associated with subsistence strategy. Underlying these investigations is the assumption that there has been a progressive reduction in dental loading; that diets have required less masticatory effort over time because of cultural preparation practices. This is supported by the appearance in the archaeological record of stone tools for grinding grains

and clay pottery for cooking at the onset of the Neolithic, which is assumed to indicate a transition to consumption of softer foods, rich in carbohydrates, such as bread and porridge. This change in diet has been explicitly associated with reduced dental macro and microwear and increased prevalence of caries in Mesolithic and Neolithic groups from different continents (Smith 1984; Molleson et al. 1993 Larsen, 1995; Kasai and Kawamura, 2001; Eshed et al. 2006; Deter, 2009; Meng et al. 2011). With this softening of diet in mind, we relate changes in morphology to changes in biomechanical performance of the mandible, to investigate the extent to which, and in what ways differences in form and in biting performance retrodict the loading that mandibles experienced in breaking down food.

With regard to morphological differences among subsistence groups, the superimposition of individual and average Mesolithic group mandibles (Fig. 2) shows that while the anterior parts of the dental row and alveolar processes differ little in form, other aspects of morphology vary more. Thus, the mandibular body is variable in height and in length such that the third molar is variably present and the earliest Upper Palaeolithic individual in the study, Oase, possesses a small retromolar space. Mandibles also vary in the width and height of the mandibular ramus as well as in the flare and flexion of the gonial angle. The PCA of size and shape and the warpings of the mean associated with each axis (Fig. 3) show that with increasing modernity, mandibles become smaller, less 'square' in gonial angle, and have a relatively shorter body and taller ramus. This last observation corresponds with that made by von Cramon Taubadell (2011) for agriculturalist vs hunter-gatherer mandibles and falsifies H_1: Mandibular form does not vary in a way that is consistent with the differences among modern subsistence groups.

These changes to large degree reflect the pattern of growth of the mandible (Enlow, 1990) in that, as the mandible grows, lengthening of the body and ramus is achieved by co-ordinated resorption at the anterior border of the ramus with deposition at its posterior border. The anterior ramal resorption progressively exposes space for the molar dentition. Modernity in our material is associated with reduced lengthening of the body and so, progressive reduction of mandibular body length and loss of the third molar. This is consistent with diminished growth relative to potential in experimental studies on animal models brought up on soft and hard diets (Hichjo et al. 2014; Bozzini et al. 2015; Kono et al. 2017) and with studies on the relationship between third molar anagenesis and mandibular body morphology in modern children (Ramiro-Verdugo et al. 2015; Celikoglu et al. 2011; Sánchez et al. 2009)

The 'modernity' of recent human jaw form results in higher efficiency of conversion of muscle to biting forces (Table 4) but strains are increased in the smaller more modern mandibles, particularly in the molar biting simulations (Fig. 5). The larger volume of the upper Palaeolithic mandibles results in less likelihood of failure. Thus, even though modern mandibles are more efficient at biting, they are relatively (muscle forces kept constant in this study, see below) less able to resist the resulting forces.

While the plots of the first pair of PCs from the PCAs of deformations (Fig. 6) show no obvious relationship between mode or magnitude of deformation and subsistence, PLS analyses (Figs. 7, 8) demonstrate that the biomechanical response of the mandible covaries with its size and shape. Therefore, H_2: Performance does not covary with mandibular form, is also falsified. In particular, smaller modern mandibles have shorter bodies and during incisor biting simulations they undergo less internal wishboning than larger ones with longer bodies and hence longer force lever arms. In turn, these differences are strongly associated with subsistence mode. Similarly during simulated M_2 biting smaller mandibles with more obtuse angles, characteristic of more modern mandibles and so softer diets wishbone more (Fig. 8a) but this association only explains 20% of the total variance in deformation; variations in mandibular size and shape not associated with diet or modernity explain the remaining variance in deformation (Fig. 8b). Therefore, H_3: Differences in performance do not reflect subsistence mode, is also falsified, particularly for more anterior bites.

Our tests assessed the extent to which mandibles varying in size and shape are more or less effective at converting muscle to biting forces and resisting those forces. We apply the same muscle force to each model to avoid confounding the effects of form on performance. In reality, as noted in the materials and methods section, each mandible would have been subject to its own specific muscle forces and as such smaller mandibles may well have been loaded less than larger ones, thus rendering strain magnitudes more similar. While interesting, the effects of varying muscle forces are not the subject of the present study. Rather, we compare performance among models loaded with the same forces in order to investigate the effects of form variation of performance. Our sample includes mandibles of Upper Palaeolithic, Mesolithic and more modern humans, with varying subsistence strategies and so histories of dental loading. If mandibles are adapted to masticatory system loading, a reasonable expectation is that when diets are less processed/softened, the resulting mandibles are better able to generate and resist high bite forces than modern mandibles that have experienced softer diets during their development. Our findings do not fit this expectation in that, for the same input force, modern mandibles generate higher bite forces but are less well

able to resist them. This suggests that they are not adapted to larger bite forces; that they habitually experienced lower than maximal bite forces. As such, increased biting efficiency is more likely a consequence of facial reduction and retraction rather than a driver of it. Modern human faces and mandibles are reduced and often fail to achieve their full growth potential because they are not subjected to high loads in childhood, paralleling the situation, described in the introduction, in experimental studies in animals fed diets of varying toughness (Ciochon et al., 1997; Lieberman et al., 2004; Menegaz et al., 2010; Ravosa et al., 2010, Hichjo et al., 2014; Bozzini et al., 2015; Kono et al., 2017)

Thus, in comparing mandibular form and function among anatomically modern humans from the Upper Palaeolithic to modern times the principal dietary signal reflects our shift to softer, more processed diets through relative under development rather than adaptation (Carlson and Van Gerven, 1977; Corruccini, 1984; González-José et al., 2005; Kaifu et al., 1997; Mays, 2015; Paschetta et al., 2010; Pinhasi and Shaw, 2008; Rando et al., 2014) This is, in turn superimposed on genetic history, climatic and other factors that also influence craniofacial form (Nicholson and Harvati, 2006). This contrasts with the comparison of mandibular form and function among groups of mammals or more ancient hominins, where the expectation is that evolutionary and ontogenetic adaptation to diets, impacts form and function in ways that can be turned to inferring dietary specialisations (Strait et al., 2009, 2010; Wroe et al., 2010) because they are adaptive. In recent humans, underdevelopment of the mandible reflects culture, not a specific diet and the archaeologist should therefore not expect to be able to make any specific dietary inferences, beyond the general level of loading.

The association between mandibular morphology and biomechanical performance in resisting deformation during biting, is not simple but the analyses we present here begin to describe it. More extensive studies, with bigger samples, simulating more bites and paramasticatory loadings are needed to fully understand how form and function intertwine. However it is likely that not all morphological differences between hunter-gatherers and modern groups affect or reflect differences in biomechanical performance pertinent to retrodicting dietary loading and so subsistence strategies. This, together with the considerations raised by findings of this study in relation to the limitations of reading subtleties of diet from modern human mandibular form and function caution that it is unlikely that morphological and functional comparisons of mandibles across cultural transitions can differentiate anything other than broad aspects of jaw loading history at a population level.

5. Acknowledgements

We would like to take this opportunity to extend our thanks to colleagues, who provided us with material access and offered invaluable feedback on this study. These include: Prof. E. Trinkaus , Washington University St Louis, Prof. A. Buzhilova from the Anuchin's Institute and Museum of Anthropology, Moscow State University, Russia; Dr A. Soficaru, Francis J. Rainer Institute of Anthropology, Romanian Academy, Bucharest. Dr. S. Vasiliev, Institute of Anthropology and Ethnology, Russian Academy of Sciences. At CAHS we have been helped and supported by various students and colleagues; Jenny Parker, Dr. Laura Fitton, Dr Sam Cobb and Dr Phil Cox.

This project could not have been conducted without the financial support of the European Commission Research Grant No. PIIF-GA-2013-622846 .

6. References

1. Bozzini, C., Picasso, E., Champin, G., Bozzini, C.E., Alippi, R.M. 2015. Effect of physical consistency of food on the biomechanical behaviour of the mandible in the growing rat. *Eur. J. Oral. Sci.* 123, 350–355.
2. Bonsall, C., Cook, G., Lennon, R., Harkness, D., Scott, M., Bartosiewicz, L., McSweeney, K., 1997. Stable isotopes, radiocarbon and the Mesolithic - Neolithic transition in the iron gates: a palaeodietary perspective. *J. Euro. Archaeol.* 5, 50-92.
3. Bonsall, C., Cook, G., Lennon, R., Harkness, D., Scott, M., Bartosiewicz, L., McSweeney, K., 2000. Stable isotopes, radiocarbon and the Mesolithic-Neolithic transition in the Iron Gates. *Documenta Praehistorica* 27, 119-132.
4. Bonsall, C., Macklin, M.G., Payton, R.W., Boroneantx, A. 2002. Climate, floods and river gods: environmental change and the meso-neolithic transition in southeast Europe. *Before Farming* 3-4, 1-15.
5. Bonsall, C., Cook, G.T., Hedges, R.E.M., Higham, T.F.G., Pickard, C., Radovanoviç, I. 2004. Radiocarbon and stable isotope evidence of dietary change from the Mesolithic to the Middle Ages in the iron gates: new results from Lepenski Vir. *Radiocarbon* 46, 293-300.
6. Carlson, S.D., Van Gerven, D.P., 1977. Masticatory function and Post-Pleistocene evolution in Nubia. *Am. J. Phys. Anthropol.* 46, 495-506.
7. Celikoglu, M., Bayram, M., NuraAm, M. 2011. Patterns of third-molar agenesis and associated dental anomalies in an orthodontic population. *J. Orthod. Dentofacial Orthop*. 140, 856-60

8. Ciochon, R.L., Nisbett, R.A., Corruccini, R.S., 1997. Dietary consistency and craniofacial development related to masticatoryfunction in minipigs. *J. Craniofac. Genet. Dev. Biol.* 17, 96–102.
9. Cook, G.T., Bonsall, C., Hedges, R.E.M., McSweeney, K., Boroneantx, V., Pettitt, P.B. 2001. A freshwater diet-derived 14C reservoir effect at the stone age sites in the iron gates Gorge. *Radiocarbon* 43, 453-460.
10. Cook, G.T., Bonsall, C., Hedges, R.E.M., McSweeney, K., Boroneantx, V., Bartosiewicz, L., Pettitt, P.B., 2002. Problems of dating human bones from the Iron Gates. *Antiquity* 76, 77-85.
11. Corruccini, R.S*.* 1984*.* An epidemiologic transition in dental occlusion in world populations. *Am. J. Orthodont.* 82, 371–376.
12. Deter, C.A. 2009. Gradients of occlusal wear in hunter-gatherers and agriculturalists*. Am. J. Phys. Anthropol.* 138, 247-254
13. Dryden I.L., Mardia K.V. 1998. *Statistical Shape Analysis.* John Wiley & Sons.
14. Enlow, D. 1990. *Facial Growth, 3rd Edition.* Saunders: Philadelphia
15. Eshed, V., Gopher, A ., Hershkovitz, I., 2006. Tooth wear and dental pathology at the advent of agriculture: New evidence from the Levant. *Am. J. Phys. Anthropol.* 130, 145-159.
16. Fitton, L. C., Prôa, M., Rowland, C., Toro-ibacache, V., & O'Higgins, P. 2015. The impact of simplifications on the performance of a finite element model of a *Macaca fascicularis* cranium. *Anat. Rec.* 298, 107-121.
17. Fu, Q., Hajdinjak, M., Moldovan, O.T., Constantin, S., Mallick, S., Skoglund, P., Patterson, N., Rohland, N., Lazaridis, I., Nickel, B., Viola, B., Prüfer,K., Meyer, M., Kelso, J., Reich, D., Pääbo, S. 2015. An early modern human from Romania with a recent Neanderthal ancestor. *Nature*. 524, 216-219 doi:10.1038/nature14558.
18. Godinho, R. M., Toro-Ibacache, V., Fitton, L. C., O'Higgins, P. 2017. Finite element analysis of the cranium: Validity, sensitivity and future directions. *C. R. Palevol* 16, 600–612.
19. González-José, R., Ramirez-Rozzi, F., Sardi, M., Martínez-Abadías, N., Hernandez, M., Pucciarelli, H.M. 2005. Functional-cranial approach to the influence of economic strategy on skull morphology. *Am. J. Phys. Anthropol.* 128, 757–771.
20. Gröning, F., Fagan, M.J., O'Higgins P. 2011a. The effects of the periodontal ligament on mandibular stiffness: a study combining finite element analysis and geometric morphometrics. *J. Biomech.* 44, 1304–1312.
21. Gröning, F., Liu, J., Fagan, M.J., O'Higgins P. 2011b. Why do humans have chins? Testing the mechanical significance of modern human symphyseal morphology with finite element analysis. *Am. J. Phys. Anthropol.* 144, 593–606.

22. Hichijo, N., Kawai, N., Mori, H., Sano R., Ohnuki Y., Okumura S., Langenbach G.E.J., Tanaka E. 2014. Effects of the masticatory demand on the rat mandibular Development, *J Oral Rehab.* 41, 581—587.
23. Hoffecker, J. 2002. Desolate landscapes: Ice-age settlement in Eastern Europe. New Brunswick, New Jersey and London: Rutgers University Press, pp. 320.
24. Jacobs, K., 1995. Returning to Oleni' ostrov: social, economic and skeletal dimensions in a boreal forest Mesolithic cemetery. *J Anthropol Archaeol* 14, 359-403.
25. Kiltie, R.A. 1984. Size ratios among sympatric neotropical cats. *Oecologia (Berl)* 61, 411–416.
26. Kaifu, Y. 1997. Changes in mandibular morphology from the Jomon to modern periods in Eastern Japan. *Am. J. Phys. Anthr.*, 104, 227-243.
27. Kasai, K., Kawamura, A. 2001. Correlation between buccolingual inclination and wear of mandibular teeth in ancient. *Arch. Oral Biol.* 46, 269–273.
28. Kono, K., Tanikawa, C., Yanagita, T., Kamioka, H., Yamashiro, T. 2017. A novel method to detect 3D mandibular changes related to soft-diet feeding. *Front. in Physiol.* 8, Article 567.
29. Larsen, C.S. 1995. Biological Changes in Human-Populations with Agriculture. *Ann. Rev. Anthr.*
30. Lieberman, D.E., Krovitz, G.E., Yates, F.W., Devlin, M., St. Claire, M. 2004. Effects of food processing on masticatory strain and craniofacial growth in a retrognathic face. *J. Hum. Evol.* 46, 655–677.
31. Lille, M., Budd, C., Potekhina, I. 2011. Stable isotope analysis of prehistoric populations from the cemeteries of the Middle and Lower Dnieper Basin, Ukraine. *J. Arch. Sci.* 38, 57-68.
32. Mays, S. 2015. Mandibular morphology in two archaeological human skeletal samples from northwest Europe with different masticatory regimes. *HOMO – J. Comparat. Hum. Biol.* 66, 203–215.
33. Menegaz, R.A, Sublett, S.V., Figueroa, S.D., Hoffman, T.J., Ravosa, M.J., Aldridge, K. 2010. Evidence for the influence of diet on cranial form and robusticity. *Anat. Rec.* 293, 630–64.
34. Menéndez, L., Bernal, V., Novellino, P., S. Perez, I. 2014. Effect of bite force and diet composition on craniofacial diversification of southern south American human populations. *Am. J. Phys. Anthr*. 155, 114–127.
35. Meng, Y., Zhang, H.Q., Pan, F., He, Z.-D., Shao, J.-L., Ding, Y., 2011. Prevalence of dental caries and tooth wear in a Neolithic population (6700-5600 years BP) from northern China. *Arch. Oral Biology* , 56, 1424-1435.
36. Milne, N., O'Higgins, P. 2012. Scaling of form and function in the xenarthran femur: a 100-fold increase in body mass is mitigated by repositioning of the third trochanter. *Proceed. R. Soc. B*. 279, 3449-3456.

37. Mitteroecker, P., Gunz, P., Windhager, S., & Schaefer, K. 2013. A brief review of shape, form, and allometry in geometric morphometrics, with applications to human facial morphology. *Hystrix*, 24, 59-66.
38. Molleson, T.I., Jones, K., Jones, S. 1993. Dietary changes and the effects of food preparation on microwear patterns in the Late Neolithic of Abu Hureyra, northern Syria. *J. Hum. Evol.* 24, 455 – 468.
39. Nicholson, E., Harvati, K., 2006. Quantitative analysis of human mandibular shape using three-dimensional geometric morphometrics. *Am. J. Phys. Anthr.* 131, 368–383.
40. Nalawade-Chawan, S., McCullagh, J., Hedges, R. 2014. New Hydroxyproline Radiocarbon Dates from Sungir, Russia, Confirm Early Mid Upper Palaeolithic Burials in Eurasia. *PLOS One*. 9, e 76896. doi:10.1371/journal.pone.0076896.
41. O'Higgins, P., Milne, N. 2013. Applying geometric morphometrics to compare changes in size and shape arising from finite elements analyses. *Hystrix*. 24, 126-132.
42. O'Higgins, P., Fitton, L. C., & Godinho, R. M. 2017. (In Press). Geometric morphometrics and finite elements analysis: Assessing the functional implications of differences in craniofacial form in the hominin fossil record. *J. Arch. Sci.* dx.doi.org/10.1016/j.jas.2017.09.011
43. O'Higgins, P., Cobb, S.N., Fitton, L.C., Gröning, F., Phillips, R., Liu, J., Fagan, M.J. 2011. Combining geometric morphometrics and functional simulation: an emerging toolkit for virtual functional analyses. *J. Anat.* 218, 3–15.
44. O'Higgins, P., Fitton, L.C., Phillips, R., Shi, JF., Liu, J., Gröning, F., Cobb S.N., Fagan, M.J. 2012. Virtual functional morphology: novel approaches to the study of craniofacial form and function. *Evol. Biol.* 39, 521-535. DOI 10.1007/s11692-012-9173-8.
45. Paschetta, C., de Azevedo, S., Castillo, L., Martínez-Abadías, N., Hernández, M., Lieberman, D.E., González-José, R. 2010. The influence of masticatory loading on craniofacial morphology: a test case across technological transitions in the Ohio Valley. *Am. J. Phys. Anthr.* 141, 297–314.
46. Pinhasi, R., Eshed, V., Shaw, P. 2008. Evolutionary changes in the masticatory complex following the transition to farming in the southern Levant. *Am. J. Phys. Anthr.* 135, 136–148.
47. Ramiro-Verdugo, J., De Vicente-Corominas, E., Montiel-Company, J.M., Gandía-Franco, J.L., Bellot-Arcís, C. 2015. Association between third molar agenesis and craniofacial structure development. *Am. J. Orthod. Dentofacial Orthop.* 148, 799-804.
48. Rando, C., Hillson, S., Antoine, A. 2014. Changes in mandibular dimensions during the mediaeval to post-mediaeval transition in London: A possible response to decreased masticatory load. *Arch. Oral Biol.* 59, 73-81.

49. Ravosa, M.J., Ning, J., Costley D.B., Daniel, A.N., Stock, S.R., Stack M.S. 2010. Masticatory biomechanics and masseter fiber-type plasticity. *J Musculoskelet Neuronal Interact*. 10, 46-55.
50. Sánchez, M.J., Vincente, A., Bravo, L.A. 2009. Third molar agenesis and craniofacial morphology. *Angle Orthod*. 79, 473–478.
51. Smith, H. 2009. Which Cranial Regions Reflect Molecular Distances Reliably in Humans? Evidence from Three-Dimensional Morphology. *Am. J. Hum. Biol.* 21, 36–47.
52. Smith, B.H. 1984. Patterns of molar wear in hunter-gatherers and agriculturalists. *Am. J. Phys. Anthr.* 63, 39–56.
53. Spassov et al., 2017. Congenital muscle dystrophy and diet consistency affect mouse skull shape differently. *J. Anat.,* 231, 736-748. doi: 10.1111/joa.12664.
54. Stansfield, E., Parker, J., O'Higgins, P. 2018. A sensitivity study of human mandibular biting simulations using finite element analysis. *J. Arch. Sci. Reports.* current issue.
55. Strait, D.S., Weber, G.W., Neubauer, S., Chalk, J., Richmond, B.G., Lucas, P.W., Spencer, M.A., Schrein, C., Dechow, P.C., Ross, C.F., Grosse, I.R., Wright, B.W., Constantino, P., Wood, B.A., Lawn, B., Hylander, W.L., Wang, Q., Byron, C., Slice, D.E., Smith, A.L., 2009. The feeding biomechanics and dietary ecology of *Australopithecus africanus*. *P. Natl. Acad. Sci. USA* 106, 2124-2129.
56. Strait, D.S., Grosse, I.R., Dechow, P.C., Smith, A.L., Wang, Q., Weber, G.W., Neubauer, S., Slice, D.E., Chalk, J., Richmond, B.G., Lucas, P.W., Spencer, M.A., Schrein, C., Wright, B.W., Byfton, C., Ross, C.F., 2010. The structural rigidity of the cranium of *Australopithecus africanus*: implications for diet, dietary adaptations, and the allometry of feeding biomechanics. *Anat. Rec.* 293, 583-593.
57. Thomason, J.J. 1991. Cranial strength in relation to estimated biting forces in some mammals. *Can. J. Zool.* 69, 2326–2333.
58. Toro-Ibacache, V., Zapata Munoz, V., & O'Higgins, P. 2015. The Predictability from Skull Morphology of Temporalis and Masseter Muscle Cross-Sectional Areas in Humans. *The Anatomical Record*. 298, 107-121
59. Toro-Ibacache, V., Muñoz, V. Z., & O'Higgins, P. 2016a. The relationship between skull morphology, masticatory muscle force and cranial skeletal deformation during biting. *Annals Anat.- Anatom. Anz.* 203, 59-68.
60. Toro-Ibacache, V., Fitton, L. C., Fagan, M. J., & O'Higgins, P. 2016b. Validity and sensitivity of a human cranial finite element model: implications for comparative studies of biting performance. *J. Anat*. 228, 70-84.
61. Von Cramon-Taubadell, N. 2011. Global human mandibular variation reflects differences in agricultural and hunter-gatherer subsistence strategies. *PNAS*. 108, 19546–19551.

62. Weijs, W.A., Hillen, B. 1986. Correlation between the cross-sectional area of the jaw muscles and craniofacial sizeand shape. *Am. J. Phys. Anthr.*. 70, 423–431.
63. Wroe, S., Ferrara, T.L., McHenry, C.R., Curnoe, D., Chamoli, U. 2010. The craniomandibular mechanics of being human. *Proc. R. Soc. B.* 277, 3579–3586.

Legends for Figures

Figure 1. Finite element model of a mandible showing muscle attachment areas (masseter, dark blue = deep, light blue =superficial; temporalis, anterior = pink, middle = red, posterior = brown; medial pterygoid = violet; lateral pterygoid = rose). Lines of action are drawn between origin and insertion, condylar and incisor constraints shown in black (see text for details).

Figure 2. Principal component analysis of the whole dataset. Given that PC1 reflects the dispersion of the sample by size, PC2 v. PC3 are presented to show separation of the groups by shape of the mandible.

Figure 3. Mandibles as per key, superimposed (translated and rotated) to best fit the anterior dentition.

Figure 4. PCA of size and shape of the mandibular sample. PC1 vs PC2, 77.4% of the total variance is displayed in this plot.

Figure 5. Von Mises strains developed in each model under simulated incisor and molar biting. See text for details.

Figure 6. a) Size and shape analysis of deformations arising from simulated biting on (a) the first right incisor: deformations are visualised as warpings of the mean unloaded model and exaggerated by a factor of 400 to aid visualisation; top left is the unloaded mean mandible, bottom left is deformation in the modern small model, bottom right is the deformation of the Sungir model, and top right is the deformation of the Oase model. b) the second right molar: deformations are visualised as warpings of the mean unloaded model and exaggerated by a factor of 400 to aid visualisation; right inset is the unloaded mean mandible, left top is the deformation in the Sungir model, left middle is the deformation in the Modern small, and left bottom is the deformation in the Modern large models. See text for details.

Figure 7. PLS of mandibular deformation arising from simulated biting on I_1 (vertical axis) vs. Mandibular size and shape (horizontal axis). The % of the total variance in deformation or form is shown on each axis The correlation between scores on these axes is r= 0.94, P= *0.0051.* Deformations are visualised as warpings of the mean unloaded model to the extremes of each PLS axis and exaggerated by a factor of 400 to aid visualisation.

Figure 8. (a) PLS axes 2 of mandibular deformation from simulated biting on M_2 (vertical axis) vs. Mandibular size and shape (horizontal axis). The % of the total variance in deformation or form is

shown on each axis. The correlation between scores on these axes is r= 0.94, P=0.004; (b) PLS axes 1 of mandibular deformation (vertical axis) vs. Mandibular size and shape (horizontal axis). The % of the total variance in deformation or form is shown on each axis. The correlation between scores on these axes is r= 0.89, P=0.017. Deformations are visualised as warpings of the mean unloaded model to the extremes of each PLS axis and exaggerated by a factor of 400 to aid visualisation.